AIMS Mathematics, 9(7): 19385–19396.
DOI: 10.3934/math.2024944
Received: 16 April 2024
Revised: 14 May 2024
Accepted: 23 May 2024
Published: 12 June 2024

https://www.aimspress.com/journal/Math

Research article

A fully-decoupled energy stable scheme for the phase-field model of non-Newtonian two-phase flows

Wei Li[1], **Guangying Lv**[1,2,*]

[1] School of Mathematics and Statistics, Nanjing University of Information Science and Technology, Nanjing 210044, China

[2] School of Mathematics and Computational Sciences, Hunan University of Science and Technology, Xiangtan, Hunan 411201, China

* **Correspondence:** Email: gylvmaths@nuist.edu.cn.

Abstract: In this paper, we first propose a novel fully-decoupled, linear and second-order time accurate scheme to solve the phase-field model of non-Newtonian two-phase flows; the developed scheme is based on a stabilized Scalar Auxiliary Variable (SAV) approach. We strictly prove the unconditional energy stability of the scheme and conduct a numerical simulation to show the accuracy and stability of the proposed scheme. Moreover, we can observe that the parameter r in non-Newtonian fluids can affect spatial patterns during phase transitions, which directly enables us to design and perform optimal control experiments in engineering processes.

Keywords: phase-field model; non-Newtonian two-phase flows; stabilized-SAV approach; unconditionally energy-stable scheme
Mathematics Subject Classification: 65M06, 65M12, 82C26

1. Introduction

In this paper, we focus on the numerical methods for a non-Newtonian fluid dynamical system coupled to the Cahn-Hilliard equation [1], which is governed by the following:

$$\begin{cases} \phi_t + \nabla \cdot (\boldsymbol{u}\phi) - \nabla \cdot (M\nabla\mu) = 0 \ \text{ in } \Omega \times (0,T), \\ \mu + \Delta\phi - f(\phi) = 0 \ \text{ in } \Omega, \\ \boldsymbol{u}_t + (\boldsymbol{u}\cdot\nabla)\boldsymbol{u} - \nabla\cdot\sigma(\boldsymbol{u}) + \nabla p + \phi\nabla\mu = 0 \ \text{ in } \Omega\times(0,T), \\ \nabla\cdot\boldsymbol{u} = 0 \ \text{ in } \Omega, \end{cases} \tag{1.1}$$

where $T > 0$, $\Omega \subset \mathbb{R}^2$ is a bounded domain, $f(\phi) = F'(\phi) = \phi^3 - \phi$, $\boldsymbol{u}$ represents the velocity, p is the pressure, μ denotes the chemical potential of the binary mixture depending on the phase function ϕ, and $M > 0$ is the mobility. Here, we consider the extra-stress tensor $\sigma(\boldsymbol{u})$ that obeys the following Carreau's law [2]:

$$\sigma(\boldsymbol{u}) = \{\nu_1 + \nu_2(1 + \kappa|D(\boldsymbol{u})|^2)^{\frac{r-2}{2}}\}D(\boldsymbol{u}), \tag{1.2}$$

where $D(\boldsymbol{u}) = (\nabla \boldsymbol{u} + \nabla \boldsymbol{u}^T)/2$ represents the strain and the parameters $\nu_1 > 0$, $\nu_2 > 0$, and $\kappa > 0$. The fluids are characterized to have a shear-thinning behavior for $1 < r < 2$ and a shear-thickening behavior for $r > 2$.

Throughout the paper, we close the aforementioned system (1.1) with the following initial and boundary conditions:

$$\begin{cases} \phi(\mathbf{x}, 0) = \phi_0, \boldsymbol{u}(\mathbf{x}, 0) = \boldsymbol{u}_0, \\ \boldsymbol{u} \cdot \boldsymbol{n}|_{\partial\Omega} = 0, \ \nabla\phi \cdot \boldsymbol{n}|_{\partial\Omega} = 0, \ M\nabla\mu \cdot \boldsymbol{n}|_{\partial\Omega} = 0, \end{cases} \tag{1.3}$$

where $x \in \Omega$ is the spatial variables, and $\boldsymbol{n}$ denotes the unit outward normal to the boundary $\partial\Omega$. Phase-field models have been widely studied by many authors. Bian-Zhang [3] established the weak solutions for a degenerate phase-field model via a Galerkin approximation. In view of a physical point, the background of the phase-field model is well studied, see [4, 5].

For the case $r = 2$ (or $\kappa = 0$) in (1.2), the system (1.1) is reduced to the phase-field models related to the Newtonian-fluid flows. As far as the author knows, for the classical phase field model of two-phase flows the only available energy-stable fully-decoupled scheme was developed in [6–8], in which a full decoupling structure was achieved by adding a stabilization term to the explicit advection velocity term. However, this decoupling type scheme is only first-order accurate in time and it requires more calculations at each time step. A second-order fully-decoupled scheme was developed in [9, 10], in which the advection and surface tension terms were discretized through explicit and implicit combination methods, which can inevitably lead to either expensive nonlinear fully-coupled schemes or relatively fast linear fully-coupled schemes. Therefore, the focus of this paper to develop a scheme for the given system that maintains an unconditionally energy stable scheme and a second-order time accuracy, while also achieving full decoupling calculations. The scalar auxiliary variable $V(t)$ is used to develop a stabilized Scalar Auxiliary Variable (SAV) approach, which has been studied by many authors in many equations such as the Allen-Cahn equation, the phase field crystal equation, and the magneto-hydrodynamic equations, see [11–13]. The reason why $V(t)$ can be used as a stabilizer is that we use the explicit format to deal with (u, ϕ), thus producing an error. In order to overcome this disadvantage, the auxiliary variable is introduced, see Lemma 2.2 for the details. Previous studies have considered a fully decoupled scheme with a stabilization term, which was essential for the phase-field model of non-Newtonian two-phase flows [14, 15]. The numerical approaches to solve the phase-field model of non-Newtonian two-phase flows contain the classical finite difference, and the finite element method, and we will provide the concrete scheme. Inspired by the works of SAV methods [16, 17] and the invariant energy quadratization (IEQ) methods [18–20], we develop a novel stabilized-SAV method to solve the coupled system (1.1). The introduction of the new auxiliary variable can provide a sufficient skill to eliminate all the troublesome nonlinear terms, which can be independently solved to achieve the fully-decoupled structure.

The rest of the paper is organized as follows. In the next section, we derive an equivalent system of the phase-field model of non-Newtonian two-phase flows with the SAV approach. In Section 3, we

propose an efficient, fully-decoupled and second-order time-accurate scheme to solve the given system. In Section 4, a numerical simulation is performed to confirm the effectiveness of the proposed method.

2. Equivalent system with the SAV approach

To begin with, in order to study the interaction of the phase-fluid interface problem, the total energy of the dynamic system is defined as a sum of the kinetic energy $E_{kin}(\boldsymbol{u})$ and the interfacial free energy $E_f(\phi)$:

$$E_{tot}[\boldsymbol{u},\phi] := E_{kin}(\boldsymbol{u}) + E_f(\phi) = \int_\Omega \frac{1}{2}|\boldsymbol{u}|^2 d\mathbf{x} + \int_\Omega (\frac{1}{2}|\nabla\phi|^2 + F(\phi))d\mathbf{x}. \tag{2.1}$$

Then, the system of phase-field models within the context of non-Newtonian fluids satisfies the following basic energy law. We say $(\phi,\mu,\boldsymbol{u},p)$ is a solution of system (1.1)–(1.3) if $(\phi,\mu,\boldsymbol{u},p)$ satisfies (1.1)–(1.3) in a weak sense.

Lemma 2.1. Let $(\phi,\mu,\boldsymbol{u},p)$ be the solution to the system (1.1)–(1.3). Then, the following energy law holds:

$$\frac{d}{dt}E_{tot}[\boldsymbol{u},\phi] + \int_\Omega \{\nu_1|D(\boldsymbol{u})|^2 + \nu_2(1+\kappa|D(\boldsymbol{u})|^2)^{\frac{r-2}{2}}|D(\boldsymbol{u})|^2 + |\sqrt{M}\nabla\mu|^2\}d\mathbf{x} = 0. \tag{2.2}$$

Moreover, suppose that the initial values $\boldsymbol{u}_0$ and ϕ_0 satisfy $E_{tot}(\boldsymbol{u}_0,\phi_0) < \infty$; then, we have the following energy dissipation law:

$$E_{tot}(\boldsymbol{u}(t),\phi(t)) \le E_{tot}(\boldsymbol{u}_0,\phi_0). \tag{2.3}$$

Proof. From (1.1)–(1.3), making use of integration by parts and using the fact that $\nabla\cdot\boldsymbol{u} = 0$, then we have the following:

$$\begin{aligned}
\frac{d}{dt}E_{tot}[\boldsymbol{u},\phi] &= \int_\Omega (\frac{\delta E_{tot}}{\delta \boldsymbol{u}}\cdot\frac{\partial \boldsymbol{u}}{\partial t} + \frac{\delta E_{tot}}{\delta\phi}\cdot\frac{\partial\phi}{\partial t})d\mathbf{x}\\
&= \int_\Omega \boldsymbol{u}\cdot\{-(\boldsymbol{u}\cdot\nabla)\boldsymbol{u} + \nabla\cdot(\nu_1 D(\boldsymbol{u})) + \nabla\cdot(\nu_2(1+\kappa|D(\boldsymbol{u})|^2)^{\frac{r-2}{2}}D(\boldsymbol{u})) - \nabla p - \phi\nabla\mu\}d\mathbf{x}\\
&\quad + \int_\Omega \mu\cdot\{-\nabla\cdot(\boldsymbol{u}\phi) + \nabla\cdot(M\nabla\mu)\}d\mathbf{x}\\
&= -\int_\Omega (\nu_1|D(\boldsymbol{u})|^2 + \nu_2(1+\kappa|D(\boldsymbol{u})|^2)^{\frac{r-2}{2}}|D(\boldsymbol{u})|^2 + |\sqrt{M}\nabla\mu|^2)d\mathbf{x},
\end{aligned} \tag{2.4}$$

where $\delta E_{tot}/\delta\phi$ denotes the variational derivative. Therefore, the proof of the desired energy law (2.2) is completed. Besides, the estimate (2.3) can be easily obtained by integrating (2.2) from 0 to t.

Remark 2.1. When deriving (2.2), it is worth noting that three nonlinear terms do not present any difficulties because they are all canceled out. More precisely, we have the following two identities:

$$\int_\Omega (\nabla\cdot(\boldsymbol{u}\phi)\mu + \phi\nabla\mu\cdot\boldsymbol{u})d\mathbf{x} = 0, \quad \int_\Omega (\boldsymbol{u}\cdot\nabla)\boldsymbol{u}\cdot\boldsymbol{u}d\mathbf{x} = 0, \tag{2.5}$$

where the first one is due to integration by parts, the second one is due to the divergence-free condition of $\boldsymbol{u}$. The two identities mean that the nonlinear terms do not contribute either to the total free energy

or the energy diffusion rate. In the next section, when developing a decoupling type scheme, we will take advantage of this often-overlooked feature of "zero-energy-contribution".

Now, we develop a stabilized-SAV approach to design a linear scheme as follows. A scalar auxiliary variable is defined by

$$V(t) = \sqrt{E(t)}, \tag{2.6}$$

with an energy function

$$E(t) = \frac{1}{2}\int_\Omega |\boldsymbol{u}|^2 d\mathbf{x} + \int_\Omega (F(\phi) - \frac{\beta}{2}\phi^2) d\mathbf{x} + C_0, \tag{2.7}$$

where β is an appropriate stabilized parameter and $C_0 > 0$ is a constant to guarantee that the radicand is positive. It is easy to check that

$$\frac{\delta V}{\delta \boldsymbol{u}} = \frac{1}{2\sqrt{E(t)}}\frac{\delta E}{\delta \boldsymbol{u}} = \frac{\boldsymbol{u}}{2V(t)}, \ \frac{\delta V}{\delta \phi} = \frac{1}{2\sqrt{E(t)}}\frac{\delta E}{\delta \phi} = \frac{H(\phi)}{2V(t)}, \tag{2.8}$$

where we denote $H(\phi) = \frac{\delta E}{\delta \phi}$. Therefore, we can rewrite the energy of (2.1) as the following formulation:

$$E_{tot}(\boldsymbol{u}, \phi; V) = \int_\Omega (\frac{1}{2}|\nabla\phi|^2 + \frac{\beta}{2}\phi^2) d\mathbf{x} + (|V(t)|^2 - C_0). \tag{2.9}$$

Based on (2.4), (2.5), and (2.6), due to $\nabla \cdot \boldsymbol{u} = 0$, then the system (1.1) can be reformulated as follows:

$$\begin{cases} \phi_t + \frac{V(t)}{\sqrt{E(t)}}\nabla\cdot(\boldsymbol{u}\phi) - \nabla\cdot(M\nabla\mu) = 0, \\ \mu + \Delta\phi - \beta\phi - H(\phi) = 0, \\ \boldsymbol{u}_t + \frac{V(t)}{\sqrt{E(t)}}(\boldsymbol{u}\cdot\nabla)\boldsymbol{u} - \nabla\cdot\sigma(\boldsymbol{u}) + \nabla p + \frac{V(t)}{\sqrt{E(t)}}\phi\nabla\mu = 0, \\ \nabla\cdot\boldsymbol{u} = 0, \\ \frac{dV(t)}{dt} = \frac{1}{2V(t)}\{\int_\Omega(\boldsymbol{u}\cdot\boldsymbol{u}_t + H(\phi)\phi_t)d\mathbf{x} \\ \quad + \frac{V(t)}{\sqrt{E(t)}}\int_\Omega(\nabla\cdot(\boldsymbol{u}\phi)\mu + \phi\nabla\mu\cdot\boldsymbol{u} + (\boldsymbol{u}\cdot\nabla)\boldsymbol{u}\cdot\boldsymbol{u})d\mathbf{x}\}, \end{cases} \tag{2.10}$$

with the following initial conditions

$$\phi(\mathbf{x}, 0) = \phi_0, \ \boldsymbol{u}(\mathbf{x}, 0) = \boldsymbol{u}_0, \ V(0) = \sqrt{E(0)}.$$

The boundary conditions in (1.3) still hold due to the new variable V, which is independent of the spatial variable.

Remark 2.2. We emphasize that the newly transformed SAV system (2.1) is exactly equivalent to the original system (2.3), since (2.6) can be easily obtained by integrating $(2.10)_5$ with respect to time. Thus, the new energy law (2.9) for the transformed system is the same as the energy law (2.1) for the original system. We state it as the following lemma.

Lemma 2.2. Let $(\phi, \mu, \boldsymbol{u}, p)$ be the solution to the system (2.10). Then, the solution satisfies the following energy dissipation law:

$$\frac{d}{dt}E_{tot}(\boldsymbol{u}, \phi; V) = -\int_{\Omega}\{\nu_1|D(\boldsymbol{u})|^2 + \nu_2(1+\kappa|D(\boldsymbol{u})|^2)^{\frac{r-2}{2}}|D(\boldsymbol{u})|^2 + |\sqrt{M}\nabla\mu|^2\}d\mathbf{x} \leq 0, \tag{2.11}$$

namely,

$$E_{tot}(\boldsymbol{u}, \phi; V) \leq E_{tot}(\boldsymbol{u}_0, \phi_0; V(0)). \tag{2.12}$$

Proof. Taking the L^2 inner product of $(2.10)_1$ with μ, $(2.10)_2$ with $-\phi_t$, $(2.10)_3$ with $\boldsymbol{u}$, $(2.10)_4$ with p, multiplying $(2.10)_5$ by $2V(t)$, and adding the resulting equations together, we directly obtain (2.11) and (2.12).

The next proposed scheme is required to formally obey the new energy dissipation law (2.9) in the discrete sense.

3. Numerical scheme

In this section, we provide a numerical scheme. The method used here has been widely studied, see [21–24] for the details. We assume a uniform partition of the time interval $[0, T]$ as $t_k = k\Delta t, k = 0, 1, \cdots, K$ with a time step $\Delta t = T/K$. For a smooth function φ, the approximation of φ at time t_k is denoted as $\varphi^k = \varphi(t_k)$. Moreover, for convenience, the following notations will be used in the sequence:

$$\phi^{k+\frac{1}{2}} = \frac{1}{2}(\phi^{k+1} + \phi^k),\ \hat{\phi}^* = \frac{3}{2}\phi^k - \frac{1}{2}\phi^{k-1},\ \widetilde{\boldsymbol{u}}^{k+\frac{1}{2}} = \frac{1}{2}(\widetilde{\boldsymbol{u}}^{k+1} + \boldsymbol{u}^k),\ \hat{\boldsymbol{u}}^* = \frac{3}{2}\boldsymbol{u}^k - \frac{1}{2}\boldsymbol{u}^{k-1}.$$

Now, it is ready to build up a numerical scheme to discretize the new system (2.8) by using the second-order Crank-Nicolson (CN) scheme. It reads as follows.

Step 1: Find $(\phi^{k+1}, \mu^{k+1}, \widetilde{\boldsymbol{u}}^{k+1})$ such that

$$\frac{\phi^{k+1} - \phi^k}{\Delta t} + \frac{V^k}{\sqrt{E^k}}\nabla\cdot(\hat{\boldsymbol{u}}^*\hat{\phi}^*) - \nabla\cdot(M\nabla\mu^{k+\frac{1}{2}}) = 0, \tag{3.1}$$

$$\mu^{k+\frac{1}{2}} + \Delta\phi^{k+\frac{1}{2}} - \beta\phi^k - H(\hat{\phi}^*) = 0, \tag{3.2}$$

$$\begin{aligned}&\frac{\widetilde{\boldsymbol{u}}^{k+1} - \boldsymbol{u}^k}{\Delta t} + \frac{V^k}{\sqrt{E^k}}(\hat{\boldsymbol{u}}^*\cdot\nabla)\hat{\boldsymbol{u}}^* + \nabla p^k + \frac{V^k}{\sqrt{E^k}}\hat{\phi}^*\nabla\hat{\mu}^* - \nabla\cdot(\nu_1 D(\widetilde{\boldsymbol{u}}^{k+\frac{1}{2}}))\\ &\quad - \nabla\cdot(\nu_2(1+\kappa|D(\hat{\boldsymbol{u}}^*)|^2)^{\frac{r-2}{2}}D(\widetilde{\boldsymbol{u}}^{k+\frac{1}{2}})) = 0.\end{aligned} \tag{3.3}$$

Step 2: Find $(\boldsymbol{u}^{k+1}, p^{k+1})$ such that

$$\frac{\boldsymbol{u}^{k+1} - \widetilde{\boldsymbol{u}}^{k+1}}{\Delta t} + \frac{1}{2}\nabla(p^{k+1} - p^k) = 0, \tag{3.4}$$

$$\nabla\cdot\boldsymbol{u}^{k+1} = 0. \tag{3.5}$$

Step 3: Update V^{k+1} as follows

$$\frac{V^{k+1}-V^k}{\Delta t}=\frac{1}{2V^{k+\frac{1}{2}}}\{\int_\Omega(\widetilde{\boldsymbol{u}}^{k+\frac{1}{2}}\cdot\frac{\boldsymbol{u}^{k+1}-\boldsymbol{u}^k}{\delta t}+H(\hat{\phi}^*)\frac{\phi^{k+1}-\phi^k}{\Delta t})d\mathbf{x}$$
$$+\frac{V^k}{\sqrt{E^k}}\int_\Omega(\nabla\cdot(\hat{\boldsymbol{u}}^*\hat{\phi}^*)\mu^{k+\frac{1}{2}}+\hat{\phi}^*\nabla\hat{\mu}^*\cdot\widetilde{\boldsymbol{u}}^{k+\frac{1}{2}}+(\hat{\boldsymbol{u}}^*\cdot\nabla)\hat{\boldsymbol{u}}^*\cdot\widetilde{\boldsymbol{u}}^{k+\frac{1}{2}})d\mathbf{x}\}. \tag{3.6}$$

The boundary conditions of the schemes (3.1)–(3.6) are given by the following:

$$\widetilde{\boldsymbol{u}}^{k+1}|_{\partial\Omega}=\boldsymbol{u}^{k+1}\cdot\boldsymbol{n}|_{\partial\Omega}=0,\ \nabla\phi^{k+1}\cdot\boldsymbol{n}|_{\partial\Omega}=0,\ M\nabla\mu^{k+1}\cdot\boldsymbol{n}|_{\partial\Omega}=0. \tag{3.7}$$

Now, the energy stability of the developed schemes (3.1)–(3.6) is shown as follows.

Theorem 3.1. The scheme (3.1)–(3.6) is unconditionally energy stable, that is, the following discrete energy law holds:

$$\mathcal{E}^{k+1}-\mathcal{E}^k=-\Delta t\|\sqrt{M}\nabla\mu^{k+\frac{1}{2}}\|^2-\nu_1\Delta t\int_\Omega|D(\widetilde{\boldsymbol{u}}^{k+\frac{1}{2}})|^2d\mathbf{x}$$
$$-\nu_2\Delta t\int_\Omega(1+\kappa|D(\hat{\boldsymbol{u}}^*)|^2)^{\frac{r-2}{2}}|D(\widetilde{\boldsymbol{u}}^{k+\frac{1}{2}})|^2d\mathbf{x}\le 0, \tag{3.8}$$

where $\mathcal{E}^{k+1}$ is the discrete version of the total energy given by the following:

$$\mathcal{E}^{k+1}=\frac{1}{2}\|\nabla\phi^{k+1}\|^2+\frac{\beta}{2}\|\phi^{k+1}\|^2+\frac{\Delta t^2}{8}\|\nabla p^{k+1}\|^2+(|V^{k+1}|^2-C_0).$$

Proof. We take the L^2-inner product of (3.1) and (3.2) with $\Delta t\mu^{k+1/2}$ and $-(\phi^{k+1}-\phi^k)$; respectively, by exploiting integration of parts and the boundary conditions (3.7) and adding the resulting equations together, we obtain the following:

$$\frac{1}{2}(\|\nabla\phi^{k+1}\|^2-\|\nabla\phi^k\|^2)+\frac{\beta}{2}(\|\phi^{k+1}\|^2-\|\phi^k\|^2)+\Delta t\|\sqrt{M}\nabla\mu^{k+\frac{1}{2}}\|^2$$
$$+\frac{\Delta tV^k}{\sqrt{E^k}}\int_\Omega\nabla\cdot(\hat{\boldsymbol{u}}^*\hat{\phi}^*)\mu^{k+\frac{1}{2}}d\mathbf{x}+\int_\Omega H(\hat{\phi}^*)(\phi^{k+1}-\phi^k)d\mathbf{x}=0. \tag{3.9}$$

By taking the L^2-inner product of (3.3) and (3.4) with $\Delta t\widetilde{\boldsymbol{u}}^{k+\frac{1}{2}}$, respectively, adding the desired results and using (3.5), one arrives at the following:

$$\int_\Omega(\boldsymbol{u}^{k+1}-\boldsymbol{u}^k)\cdot\widetilde{\boldsymbol{u}}^{k+\frac{1}{2}}d\mathbf{x}+\nu_1\Delta t\int_\Omega|D(\widetilde{\boldsymbol{u}}^{k+\frac{1}{2}})|^2d\mathbf{x}+\nu_2\Delta t\int_\Omega(1+\kappa|D(\hat{\boldsymbol{u}}^*)|^2)^{\frac{r-2}{2}}|D(\widetilde{\boldsymbol{u}}^{k+\frac{1}{2}})|^2d\mathbf{x}$$
$$-\frac{\Delta t}{4}(p^{k+1}+p^k,\nabla\cdot\widetilde{\boldsymbol{u}}^{k+1})+\frac{\Delta tV^k}{\sqrt{E^k}}\int_\Omega(\hat{\boldsymbol{u}}^*\cdot\nabla)\hat{\boldsymbol{u}}^*\cdot\widetilde{\boldsymbol{u}}^{k+\frac{1}{2}}d\mathbf{x}$$
$$+\frac{\Delta tV^k}{\sqrt{E^k}}\int_\Omega\hat{\phi}^*\nabla\hat{\mu}^*\cdot\widetilde{\boldsymbol{u}}^{k+\frac{1}{2}}d\mathbf{x}=0. \tag{3.10}$$

By taking the inner product of (3.4) with $\frac{\Delta t^2}{4}\nabla(p^{k+1}+p^k)$ in the L^2 space and using (3.5) again, we have

$$\frac{\Delta t}{4}(\nabla\cdot\widetilde{\boldsymbol{u}}^{k+1},p^{k+1}+p^k)+\frac{\Delta t^2}{8}(\|\nabla p^{k+1}\|^2-\|\nabla p^k\|^2)=0. \tag{3.11}$$

We multiply (3.6) with $2\delta t V^{k+1/2}$ to obtain the following:

$$|V^{k+1}|^2 - |V^k|^2 = \int_\Omega (\widetilde{\boldsymbol{u}}^{k+\frac{1}{2}} \cdot (\boldsymbol{u}^{k+1} - \boldsymbol{u}^k) d\mathbf{x} + \int_\Omega H(\hat{\phi}^*)(\phi^{k+1} - \phi^k) d\mathbf{x}$$
$$+ \frac{\Delta t V^k}{\sqrt{E^k}} \int_\Omega (\nabla \cdot (\hat{\boldsymbol{u}}^* \hat{\phi}^*) \mu^{k+\frac{1}{2}} + \hat{\phi}^* \nabla \hat{\mu}^* \cdot \widetilde{\boldsymbol{u}}^{k+\frac{1}{2}} + (\hat{\boldsymbol{u}}^* \cdot \nabla) \hat{\boldsymbol{u}}^* \cdot \widetilde{\boldsymbol{u}}^{k+\frac{1}{2}}) d\mathbf{x}. \tag{3.12}$$

Summing the above equations (3.9)–(3.12) together leads to the proof of the desired result (3.8). The proof is completely finished.

4. Numerical result

In this section, we aim to investigate the performance of our proposed method for the non-Newtonian two-phase flow. The solution of the systems (1.1)–(1.3) shall be a sought subject to the following initial conditions:

$$\phi_0 = \tanh\left(\frac{\sqrt{(x-0.55)^2 + (y-0.35)^2}}{\sqrt{2}\varepsilon}\right), \ \boldsymbol{u}_0 = 0,$$

where $\tanh(x) = (e^x - e^{-x})/(e^x + e^{-x})$ and $\varepsilon = 0.02$. The boundary conditions are $\phi|_{\partial\Omega} = \mathbf{u}_{\partial\Omega} = 0$.

We set the computational domain $\Omega = [0, 2]^2$ and use the finite element method to discretize the space variables (using P_2 for ϕ and $P_2 - P_1$ for $(\mathbf{u}, p)$); the parameters are given as $M = 1, \nu_1 = 0.03, \nu_2 = 0.01$, and $\kappa = 1$. Figure 1 shows the L^2 errors of the phase-field variable, the fluid velocity, the pressure between the numerical solution, and the "exact solution" (which is computed by a very small time step $\delta t = 1/2^{14}$) at time $t = 0.8$ with a different r. We can see that the obtained temporal convergence rate is $O(\Delta t^2)$.

In the next simulation, we take the temporal step as $\Delta t = 0.01$ in the computations. In Figure 2(a), the evolution of the total energy curves with different parameters r is plotted, from which it is easy to see that the energy is decreasing in time, which is in a good agreement with the theoretical results (see Theorem 3.1). Figure 2(b) exhibits the pressure profile at a cross section $y = 1.0$ along the x-axis at time $t = 0.20$. Moreover, one can clearly see that the parameters r can affect the profile of the pressure, which gives rise to different patterns of the phase field. Figure 3 displays the snapshots of the phase field variable ϕ and the flow velocity vector $\boldsymbol{u}$ at the same time nodes, where the different patterns are observed under different values of r, that is, the parameter r in non-Newtonian fluids can affect the spatial shapes of a substance during a surface phase transition. Subsequently, this gives us a means to design and perform optimal control experiments for the geometric shapes of materials in engineering practice.

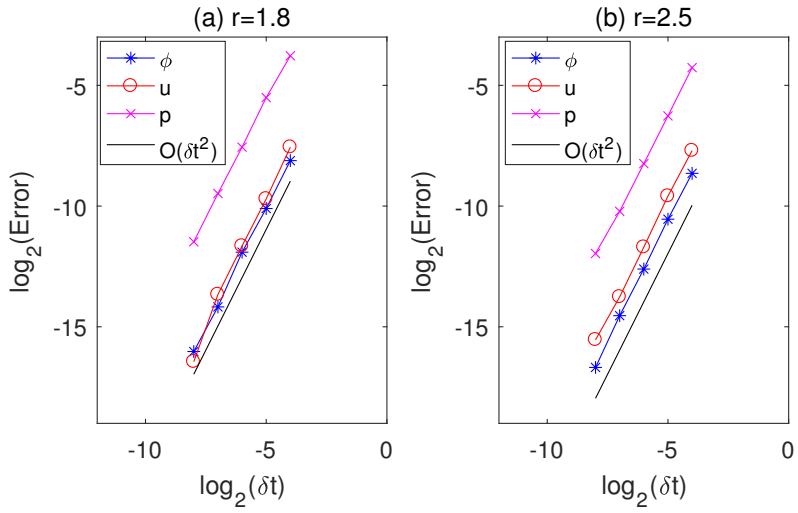

Figure 1. The L^2 errors of the phase-field variable ϕ, fluid velocity $\boldsymbol{u}$ and pressure p with different r.

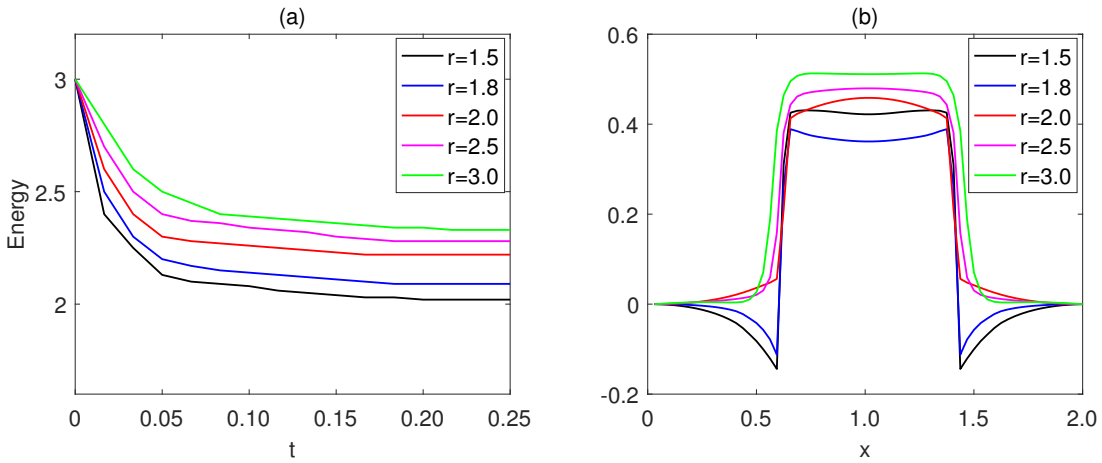

Figure 2. (a) Total energy over time for the non-Newtonian flow scenario with different parameters r. (b) Pressure profile at a cross section $y = 1.0$ along the x-axis and at time $t = 0.20$.

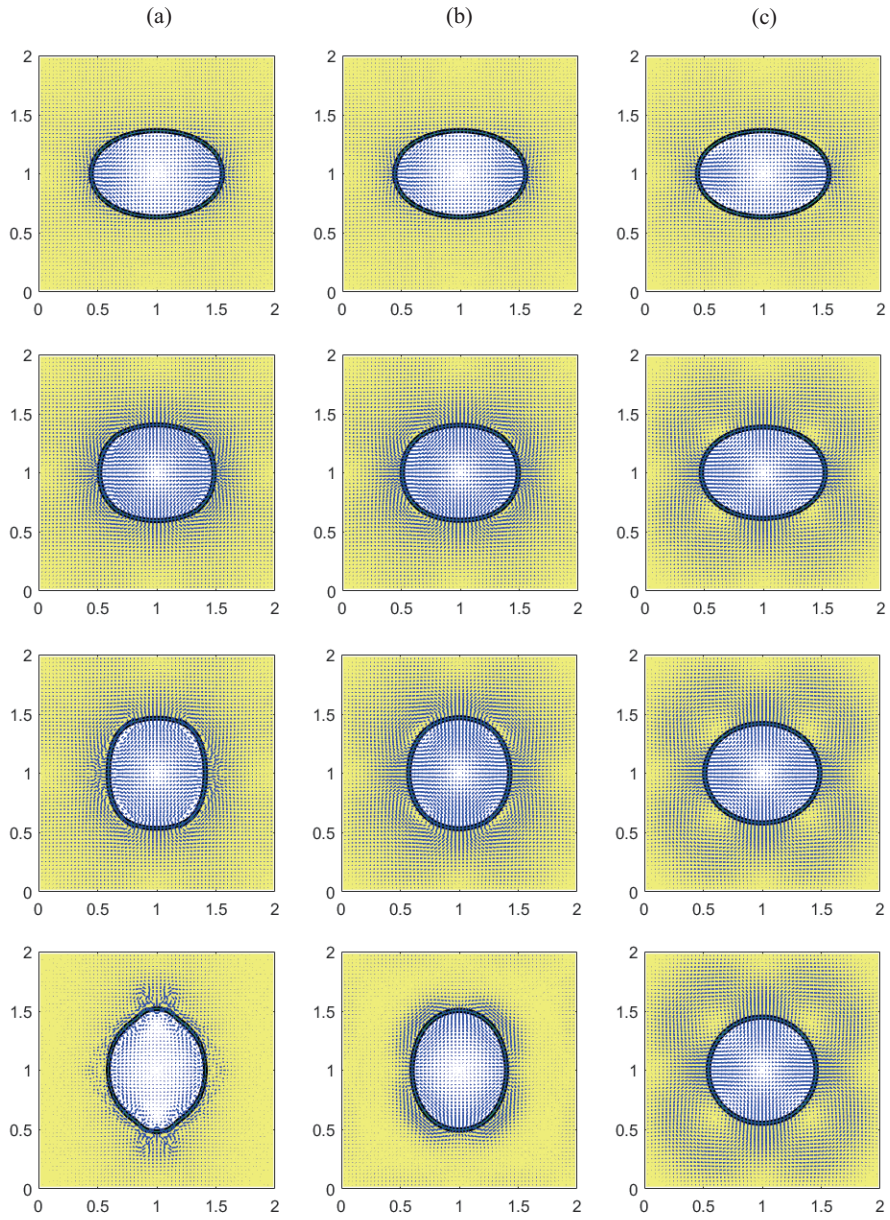

Figure 3. Snapshots of the computed phase function ϕ (dark circle denotes ϕ) and the flow velocity vector $\boldsymbol{u}$ (blue arrows denote the vector $\boldsymbol{u}$) at time $t = 0.01, 0.08, 0.14, 0.20$. For the cases with (a) $r = 1.5$, (b) $r = 2.0$, (c) $r = 3.0$, the graphs are arranged column-wise.

5. Conclusions

In this paper, a novel fully-decoupled, linear and second-order time accurate scheme to solve the phase-field model of non-Newtonian two-phase flows was introduced. The developed scheme was based on a stabilized SAV approach.

For the classical phase-field model of two-phase flows, the only available energy-stable fully-decoupled scheme was developed and a fully-decoupled structure was achieved by adding a stabilization term to the explicit advection velocity term. However, this decoupling type scheme was

only first-order accurate in time and it required more calculations at each time step. For the second-order fully-decoupled scheme, the advection and surface tension terms were discretized through explicit and implicit combination method, which can inevitably lead to either expensive nonlinear fully-coupled schemes or relatively fast linear fully-coupled schemes. Therefore, the focus of this paper was developing a scheme for the given system that maintained a unconditionally energy stable scheme and a second-order time accuracy, while also achieving fully-decoupled calculations. We strictly proved the unconditional energy stability of the scheme and conducted numerical simulations to show the accuracy and stability of the proposed scheme. Moreover, we observed that the parameter r in non-Newtonian fluids could affect spatial patterns during phase transitions, which directly enabled us to design and perform optimal control experiments in engineering processes.

Author contributions

Wei Li: Conceptualization, Investigation, Writing-original draft; Guangying Lv: Conceptualization, Validation, Writing-original draft, Writing-review and editing. All authors have read and approved the final version of the manuscript for publication.

Use of AI tools declaration

The authors declare they have not used Artificial Intelligence (AI) tools in the creation of this article.

Acknowledgments

This work was supported by the NSF of China grants 12171247, 11771123, Jiangsu Provincial Double-Innovation Doctor Program JSSCBS20210466 and Qing Lan Project, and Postgraduate Research and Practice Innovation Program of Jiangsu Province (No. KYCX21 0932).

Conflict of interest

The authors declare that they have no conflict of interest.

References

1. H. Abels, L. Diening, Y. Terasawa, Existence of weak solutions for a diffuse interface model of non-Newtonian two-phase flows, *Nonlinear Anal. Real World Appl.,* **15** (2014) 149–157. http://dx.DOI10.1016/j.nonrwa.2013.07.001
2. J. B. Barrett, W. B. Liu, Quasi-norm error bounds for the finite element approximation of a non-Newtonian flow, *Numer. Math.,* **68** (1994), 437–456. https://doi.org/10.1007/s002110050071
3. X. Bian, L. Zhao, Weak solutions for a degenerate phase-field model via Galerkin approximation, *Math. Methods Appl. Sci.,* **47** (2024), 5441–5460. https://doi.10.1002/mma.9872
4. J. Schröder, M. Pise, D. Brands, G. Gebuhr, S. Anders, Phase-field modeling of fracture in high performance concrete during low-cycle fatigue: Numerical calibration and experimental validation, *Comput. Method. Appl. M.,* **398** (2022), 115181. https://doi.10.1016/j.cma.2022.115181

5. M. Pise, G. Gebuhr, D. Brands, J. Schröder, S. Anders, Phase-field modeling for failure behavior of reinforced ultra-high performance concrete at low cycle fatigue, *Proceed. Appl. Math. Mech.,* **23** (2023), e202300233. https://doi.10.1002/pamm.202300233
6. J. Shen, X. Yang, A phase-field model and its numerical approximation for two-phase incompressible flows with different densities and viscositites, *SIAM J. Sci. Comput.,* **32** (2010), 1159–1179. https://doi.org/10.1137/09075860X
7. J. Shen, X. Yang, Decoupled energy stable schemes for phase field models of two phase complex fluids, *SIAM J. Sci. Comput.,* **36** (2014), 122–145. https://doi.org/10.1137/13092159
8. S. Minjeaud, An unconditionally stable uncoupled scheme for a triphasic Cahn-Hilliard/Navier-Stokes model, *Numer. Meth. Part. D. E.,* **29** (2013), 584–618. https://doi.org/10.1002/num.21721
9. D. Han, X. Wang, A second order in time, uniquely solvable, unconditionally stable numerical scheme for Cahn-Hilliard-Navier-Stokes equation, *J. Comput. Phys.,* **290** (2015), 139–156. https://doi.org/10.1016/j.jcp.2015.02.046
10. X. Yang, H. Yu, Efficient second order unconditionally stable schemes for a phase field moving contact line model using an invariant energy quadratization approach, *SIAM J. Sci. Comput.,* **40** (2018), B889–B914. https://doi.org/10.1137/17M1125005
11. Y. Tang, The stabilized exponential-SAV approach for the Allen-Cahn equation with a general mobility, *Appl. Math. Lett.,* **152** (2024), Paper No. 109037, 6. https://doi.org/10.1016/j.aml.2024.109037
12. F. Zhang, H. Sun, S. Tao, Efficient and unconditionally energy stable exponential-SAV schemes for the phase field crystal equation, *Appl. Math. Comput.,* **470** (2024), Paper No. 128592, 20. https://doi.org/10.1016/j.amc.2024.128592
13. X. Li, W. Wang, J. Shen, Stability and error analysis of IMEX SAV schemes for the magneto-hydrodynamic equations, *SIAM J. Numer. Anal.,* **60** (2022), 1026-1054. https://doi.org/10.1137/21M1430376
14. Y. Tang, G. Zou, J. Li, Unconditionally energy-stable finite element scheme for the chemotaxis-fluid system, *J. Sci. Comput.,* **95** (2023), Paper No. 1, 34. https://doi.org/10.1007/s10915-023-02118-4
15. X. Li, J. Shen, On fully decoupled MSAV schemes for the Cahn-Hilliard-Navier-Stokes model of two-phase incompressible flows. *Math. Models Methods Appl. Sci.,* **32** (2022), 457–495. https://doi.org/10.1142/S0218202522500117
16. X. Li, J. Shen, Error analysis of the SAV-MAC scheme for the Navier-Stokes equations, *SIAM J. Numer. Anal.,* **58** (2020), 2465–2491. https://doi.org/10.1137/19M1288267
17. J. Shen, J. Xu, Convergence and error analysis for the scalar auxiliary variable (SAV) schemes to gradient flows, *SIAM J. Numer. Anal.,* **56** (2018), 2895–2912. https://doi.org/10.1137/17M1159968
18. X. Yang, A new efficient fully-decoupled and second-order time-accurate scheme for Cahn-Hilliard phase-field model of three-phase incompressible flow, *Comput. Methods Appl. Mech. Engrg.,* **376** (2021), 113589. https://doi.org/10.1016/j.cma.2020.113589

19. X. Yang, A novel fully-decoupled, second-order and energy stable numerical scheme of the conserved Allen-Cahn type flow-coupled binary surfactant model, *Comput. Method. Appl. M.,* **373** (2021), 113502. https://doi.org/10.1016/j.cma.2020.113502

20. X. Yang, Efficient and energy stable scheme for the hydrodynamically coupled three components Cahn-Hilliard phase-field model using the stabilized-Invariant Energy Quadratization (S-IEQ) Approach, *J. Comput. Phys.,* **438** (2021), 110342. https://doi.org/10.1016/j.jcp.2021.110342

21. J. Shen, X. Yang, Energy stable schemes for Cahn-Hilliard phase-field model of two-phase incompressible flows, *Chinese Ann. Math. Ser. B*, **31** (2010), 743–758. https://doi.org/10.1007/s11401-010-0599-y

22. J. Shen, X. Yang, A phase-field model and its numerical approximation for two-phase incompressible flows with different densities and viscosities, *SIAM J. Sci. Comput.,* **32** (2010), 1159–1179. https://doi.org/10.1137/09075860

23. Y. Cai, H. Choi, J. Shen, Error estimates for time discretizations of Cahn-Hilliard and Allen-Cahn phase-field models for two-phase incompressible flows, *Numer. Math.,* **137** (2017), 417–449. https://doi.org/10.1007/s00211-017-0875-9

24. Y. Cai, J. Shen, Error estimates for a fully discretized scheme to a Cahn-Hilliard phase-field model for two-phase incompressible flows, *Math. Comp.,* **87** (2018), 2057–2090. https://doi.org/10.1090/mcom/3280

AIMS Press